

# Circulating current derivation and comprehensive compensation of cascaded STATCOM under asymmetrical voltage conditions

ISSN 1751-8687

Received on 13th November 2015

Revised on 11th April 2016

Accepted on 26th April 2016

doi: 10.1049/iet-gtd.2015.1374

www.ietdl.org

He Zhixing<sup>1</sup> ✉, Ma Fujun<sup>1</sup>, Luo An<sup>1</sup>, Xu Qianming<sup>1</sup>, Chen Yandong<sup>1</sup>, Xiao Huagen<sup>2</sup>, Jin Guobin<sup>3</sup>

<sup>1</sup>College of Electrical and Information Engineering, Hunan University, Changsha 410082, Hunan Province, People's Republic of China

<sup>2</sup>College of Information and Electrical Engineering, Hunan University of Science and Technology, Xiangtan 411201, Hunan Province, People's Republic of China

<sup>3</sup>Electrical Engineering College, Northeast Dianli University, Jilin 132012, Jilin Province, People's Republic of China

✉ E-mail: 506396463@qq.com

**Abstract:** Cascaded static synchronous compensator (STATCOM) with delta-connected configuration is an effective solution to compensate reactive and negative-sequence currents. This study focuses on the circulating current and compensation method of delta-connected STATCOM under asymmetrical voltage conditions. According to the phasor analysis, constraints of voltage phasors and current phasors under reactive current compensation mode, negative-sequence current compensation mode and comprehensive compensation mode are deduced. On the basis of this, the analytical expressions of circulating current under the three modes are derived. Furthermore, a comprehensive compensation method for delta-connected STATCOM is proposed. In the proposed method, phase current references are calculated directly with the instantaneous voltage and current signals, which could enhance the dynamic behaviour and cluster-balancing control performance especially under asymmetrical voltage conditions. Finally, simulation and experiment results have been given to verify the effectiveness and feasibility of the proposed control method.

## 1 Introduction

The static synchronous compensator (STATCOM) using voltage-source converter has been widely utilised to correct power factor (PF), to compensate unbalanced loads and enhance voltage stability in distribution and transmission grid [1–3]. With the development of power electronics technology, various topologies of multilevel converters have been proposed [4, 5]. Among these, the cascaded H-bridge multilevel converter has been an attractive topology for STATCOM in middle/high voltage grid due to its advantages such as: transformer-less, modularisation structure and desirable output performance [6–8].

Several H-bridge modules are linked in series to produce desired output voltage in cascaded STATCOM. Therefore, some pulse-width modulation (PWM) strategies have been investigated in the literatures such as: carrier-based PWM [9], selective harmonic elimination PWM [10], multilevel space vector modulation [11]. Furthermore, various investigations have also been carried out to improve output performance, to simplify control scheme and to solve practical problems [12–21]. Three-phase STATCOM can be connected in two kinds of typical topology structure: star-connected structure and delta-connected structure. The delta-connected STATCOM is easy to implement individual phase control, and also has compensation ability for negative sequence. The study of this paper will focus on delta-connected STATCOM.

In [17, 18], power compensation theory for STATCOM was illustrated in detail. In [19, 20], the decoupled current control scheme based on  $dq$  frame was proposed. In [21], a new reactive current reference algorithm was presented to improve the dynamic performance. As the dc-link capacitor of each H-bridge module is separate and isolated, the voltage balancing control of each H-bridge module and each cluster is a critical issue for cascaded STATCOM. In [22, 23], individual voltage balancing control was proposed. A bias voltage, which was obtained from voltage difference of each H-bridge module, was added to the voltage

reference of each module. In [24, 25], a hierarchical balancing control strategy was developed, then three cascaded loops of voltage balancing control: namely, overall balancing control, cluster-balancing control and individual balancing control, were investigated to regulate capacitor voltages. Furthermore, voltage balancing control of each cluster becomes more complex when STATCOM operated in unbalanced condition, because the active power produced in each phase cluster is asymmetrical [26, 27]. To solve this problem, individual phase instantaneous current control strategy was discussed in [28, 29], as the complex decomposition of positive, negative and zero-sequence component was avoided, this approach was simple. It can be known from [30] that the circulating current only flows inside the triangular, and it can be treated as an extra control freedom of STATCOM to redistribute active power among three clusters. Furthermore, three proportional and integral (PI) controllers were employed in cluster-balancing control loop to calculate the reference of circulating current. In [31, 32], the phase-cluster power balance problem was discussed and the circulating current was solved based on the power expressions of three-phase clusters. However, the derivation of circulating current in [31] was carried out under balanced voltage condition. The unbalanced voltage was taken into account in [32], but the circulating current expression was valid under conditions of voltage magnitude unbalanced only.

In this paper, first, the relationship between phase current and line current of delta-connected STATCOM under asymmetrical voltage conditions is analysed. By analysing the constrain relation of unbalanced voltage and current phasors, the analytical expression of circulating current is derived, which is valid under conditions of voltage magnitude and phase angle unbalanced. Moreover, a comprehensive compensation method for delta-connected STATCOM is proposed. Since the phase current references are calculated directly with the instantaneous voltage and current signals, this method could improve the performance of compensation and cluster-balancing control especially under

asymmetrical voltage conditions. The rest of this paper is organised as follows. Relationship between phase current and line current under unbalanced conditions is analysed in Section 2. The expression of circulating current is derived in Section 3. The comprehensive compensation method is presented in Section 4. Simulation and experiment results are presented in Section 5. Conclusions are drawn in Section 6.

## 2 Constrain relations of phase current and line current

A delta-connected cascaded STATCOM system is depicted in Fig. 1, each cluster is cascaded by H-bridge modules,  $Z_s$  is the equivalent inductance of the power grid. Here,  $u_a, u_b, u_c$  are the phase voltages of coupling point,  $i_{sa}, i_{sb}, i_{sc}$  are currents of grid side,  $i_{la}, i_{lb}, i_{lc}$  are load currents,  $i_a, i_b, i_c$  are line currents and  $i_{ab}, i_{bc}, i_{ca}$  are phase currents of STATCOM and  $i_0$  is the circulating current.

According to Song and Liu [29] and Yuan and Xia [33], under asymmetrical voltage condition, line voltages of coupling point can be described as

$$\begin{cases} u_{ab} = \sqrt{3}(U^+ \sin(\omega t + \pi/6) + U^- \sin(\omega t + \theta - \pi/6)) \\ u_{bc} = \sqrt{3}(U^+ \sin(\omega t - \pi/2) + U^- \sin(\omega t + \theta + \pi/2)) \\ u_{ca} = \sqrt{3}(U^+ \sin(\omega t + 5\pi/6) + U^- \sin(\omega t + \theta - 5\pi/6)) \end{cases} \quad (1)$$

where  $U^+$  is the amplitude of positive-sequence voltage,  $U^-$  and  $\theta$  are the amplitude and phase angle of negative-sequence voltage, respectively. The delta-connected cascaded STATCOM is utilised to compensate positive-sequence reactive and negative-sequence currents, the line currents can be expressed as

$$\begin{cases} i_a = I_q^+ \sin(\omega t + \pi/2) + I^- \sin(\omega t + \varphi) \\ i_b = I_q^+ \sin(\omega t - \pi/6) + I^- \sin(\omega t + \varphi + 2\pi/3) \\ i_c = I_q^+ \sin(\omega t + 7\pi/6) + I^- \sin(\omega t + \varphi - 2\pi/3) \end{cases} \quad (2)$$

where  $I_q^+$  is the amplitude of positive-sequence reactive current,  $I^-$  and  $\varphi$  are the amplitude and phase angle of negative-sequence current, respectively.

On the basis of (1) and (2), instantaneous dc active power of each cluster can be calculated. It is worth mentioning that the summation of dc power produced by negative-sequence voltage and negative-sequence current is not zero. To keep total power balanced, additional positive-sequence active currents  $i_{ad}^+, i_{bd}^+$ , and  $i_{cd}^+$  should be introduced in line currents when negative-sequence

current is compensated and  $I_d^+$  is the amplitude

$$\begin{cases} i_{ad}^+ = I_d^+ \sin(\omega t) \\ i_{bd}^+ = I_d^+ \sin(\omega t - 2\pi/3) \\ i_{cd}^+ = I_d^+ \sin(\omega t + 2\pi/3) \end{cases} \quad (3)$$

For delta-connected STATCOM, phase currents are always taken as the control variables. However, the transformation matrix of line current to phase current is a non-full rank, and multi-group solutions can be solved. If introducing the circulating current as a constraint of phase currents [30]

$$i_{ab} + i_{bc} + i_{ca} = 3i_0 \quad (4)$$

The only solution of phase currents  $i_{ab}, i_{bc}, i_{ca}$  is obtained

$$\begin{bmatrix} i_{ab} \\ i_{bc} \\ i_{ca} \end{bmatrix} = \begin{bmatrix} 1/3 & -1/3 & 0 \\ 0 & 1/3 & -1/3 \\ -1/3 & 0 & 1/3 \end{bmatrix} \begin{bmatrix} i_a \\ i_b \\ i_c \end{bmatrix} + \begin{bmatrix} i_0 \\ i_0 \\ i_0 \end{bmatrix} \quad (5)$$

Substituting (2) and (3) into (5), phase currents can be written as

$$\begin{bmatrix} i_{ab} \\ i_{bc} \\ i_{ca} \end{bmatrix} = \frac{\sqrt{3}}{3} \begin{bmatrix} I_d^+ \sin(\omega t + \pi/6) \\ I_d^+ \sin(\omega t - \pi/2) \\ I_d^+ \sin(\omega t + 5\pi/6) \end{bmatrix} + \frac{\sqrt{3}}{3} \begin{bmatrix} I_q^+ \sin(\omega t + 2\pi/3) \\ I_q^+ \sin \omega t \\ I_q^+ \sin(\omega t - 2\pi/3) \end{bmatrix} + \frac{\sqrt{3}}{3} \begin{bmatrix} I^- \sin(\omega t - \pi/6 + \varphi) \\ I^- \sin(\omega t + \pi/2 + \varphi) \\ I^- \sin(\omega t - 5\pi/6 + \varphi) \end{bmatrix} + \begin{bmatrix} i_0 \\ i_0 \\ i_0 \end{bmatrix} \quad (6)$$

From (6), the phase currents can be divided into four parts: positive-sequence active and reactive components, negative-sequence component and zero-sequence component. Among them, positive-sequence reactive and negative-sequence components are determined by the loads. Nevertheless, both the positive-sequence active and the zero-sequence components are related to the line currents and voltages, which will be analysed in Section 3 deeply.

## 3 Derivation of circulating current under three compensation modes

According to (2), line current phasors can be divided into positive-sequence reactive currents  $I_{aq}^+, I_{bq}^+, I_{cq}^+$  and negative-sequence currents  $I_a^-, I_b^-, I_c^-$ . Phase voltage phasors can also be divided into positive- and negative-sequence voltages  $U_a^+, U_b^+, U_c^+$  and  $U_a^-, U_b^-, U_c^-$ , respectively. The phasors diagram of phase voltage and line current is shown in Fig. 2a.

According to (1), setting  $U_d^+ = U^+$ ,  $U_d^- = U^- \cos \theta$ ,  $U_q^- = U^- \sin \theta$ ; the line voltage phasors can be expressed as

$$\begin{cases} U_{ab} = \frac{\sqrt{3}}{2}((\sqrt{3}U_d^+ + \sqrt{3}U_d^- + U_q^-) + j(U_d^+ - U_d^- + \sqrt{3}U_q^-)) \\ U_{bc} = \sqrt{3}(-U_q^- + j(-U_d^+ + U_d^-)) \\ U_{ca} = \frac{\sqrt{3}}{2}((U_q^- - \sqrt{3}U_d^+ - \sqrt{3}U_d^-) + j(U_d^+ - U_d^- - \sqrt{3}U_q^-)) \end{cases} \quad (7)$$

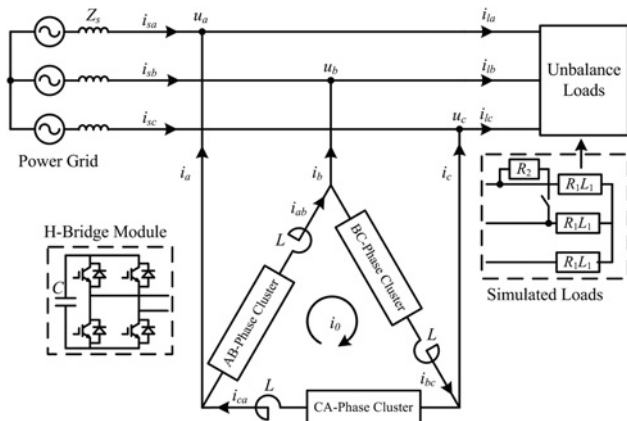
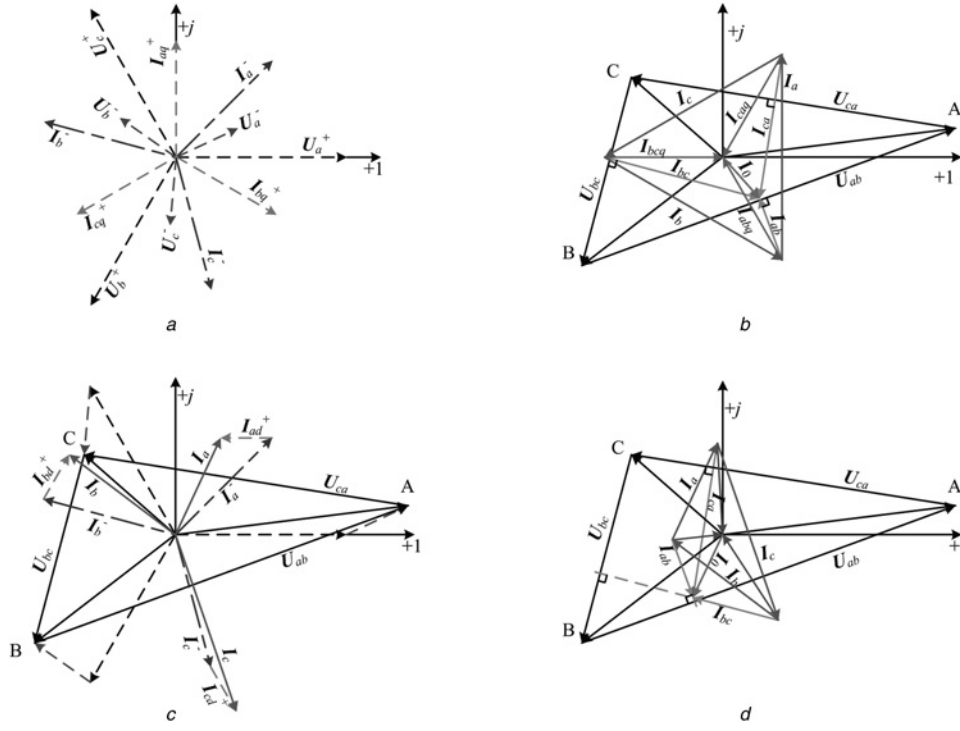


Fig. 1 Schematic configuration of delta-connected cascaded STATCOM



**Fig. 2** Phasor diagram of voltage and current

- a Phasors diagram of phase voltage and line current
- b Phasor diagram for reactive current compensation
- c Phasor diagram of voltage and line current
- d Phasor diagram for negative-sequence current compensation

Setting the circulating current phasor  $I_0$  is

$$I_0 = X + jY \quad (8)$$

In this paper, the three operational modes of delta-connected STATCOM are discussed. Therefore, the derivation of circulating current phasor  $I_0$  are carried out in the three compensation modes.

### 3.1 Reactive current compensation

Phasor diagram of this mode is shown in Fig. 2b.  $I_a, I_b, I_c$  are the line current phasors,  $I_{abq}, I_{bcq}, I_{caq}$  are the positive-sequence reactive components of phase current phasors. Since phasors  $I_{abq}, I_{bcq}, I_{caq}$  and line voltage phasors  $U_{ab}, U_{bc}, U_{ca}$  are non-orthogonal as shown in Fig. 2b, it would lead to that clusters of STATCOM absorb or release active power continuously, and even dc-link voltages being out of control. Circulating current can be introduced to redistribute active power [30]. After adding a proper circulating current  $I_0$  to  $I_{abq}, I_{bcq}, I_{caq}$ , phase current phasors  $I_a, I_b, I_c$  become orthogonal with  $U_{ab}, U_{bc}, U_{ca}$ , respectively, as shown in Fig. 2b.

Combining (2), (5) and (8),  $I_a, I_b, I_c$  can be expressed as

$$\begin{bmatrix} I_a \\ I_b \\ I_c \end{bmatrix} = \begin{bmatrix} -\frac{\sqrt{3}}{6}I_q^+ + X \\ \frac{\sqrt{3}}{3}I_q^+ + X \\ -\frac{\sqrt{3}}{6}I_q^+ + X \end{bmatrix} + j \begin{bmatrix} \frac{1}{2}I_q^+ + Y \\ Y \\ -\frac{1}{2}I_q^+ + Y \end{bmatrix} \quad (9)$$

If an appropriate circulating current  $I_0$  is selected,  $I_a, I_b, I_c$  can be

vertical with  $U_{ab}, U_{bc}, U_{ca}$ , respectively

$$\begin{cases} I_a \perp U_{ab} \\ I_b \perp U_{bc} \\ I_c \perp U_{ca} \end{cases} \quad (10)$$

According to (10), there is

$$\begin{cases} U_q^- I_q^+ + \sqrt{3}U_q^- X - (\sqrt{3}U_d^- - \sqrt{3}U_d^+)Y = 0 \\ U_d^- I_q^+ - (\sqrt{3}U_d^+ + \sqrt{3}U_d^-)X - \sqrt{3}U_q^- Y = 0 \end{cases} \quad (11)$$

Therefore, the expression of circulating current phasor  $I_0$  can be obtained as follows

$$I_0 = \frac{I_q^+(U_d^- U_d^- - U_d^+ U_d^+ - U_q^- U_q^-)}{\sqrt{3}(U_d^- U_d^- - U_d^+ U_d^+ + U_q^- U_q^-)} + j \frac{I_q^+(U_d^- U_q^- + U_d^+ U_q^- + U_d^+ U_q^-)}{\sqrt{3}(U_d^- U_d^- - U_d^+ U_d^+ + U_q^- U_q^-)} \quad (12)$$

### 3.2 Negative-sequence current compensation

Phasor diagram of this mode is shown in Figs. 2c and d. In this mode, additional positive-sequence active currents should be introduced to keep total dc power balanced. As shown in Fig. 2c, after adding the positive-sequence active currents  $I_{ad}^+, I_{bd}^+, I_{cd}^+$  to  $I_a, I_b, I_c$ , line current phasors  $I_a, I_b, I_c$  are obtained.

On the basis of the phasors  $I_a, I_b, I_c$  obtained in Fig. 2c, phasor diagram of phase current and line voltage is shown in Fig. 2d. As shown in Fig. 2d, a suitable circulating current phasor  $I_0$  can be solved, when it is added to the three-phase current phasors,  $I_a, I_b, I_c$  can be orthogonal to  $U_{ab}, U_{bc}, U_{ca}$ , respectively. Assuming  $I_d^- = I^- \cos \varphi, I_q^- = I^- \sin \varphi$ , combining (2), (3), (5) and (8),  $I_a,$

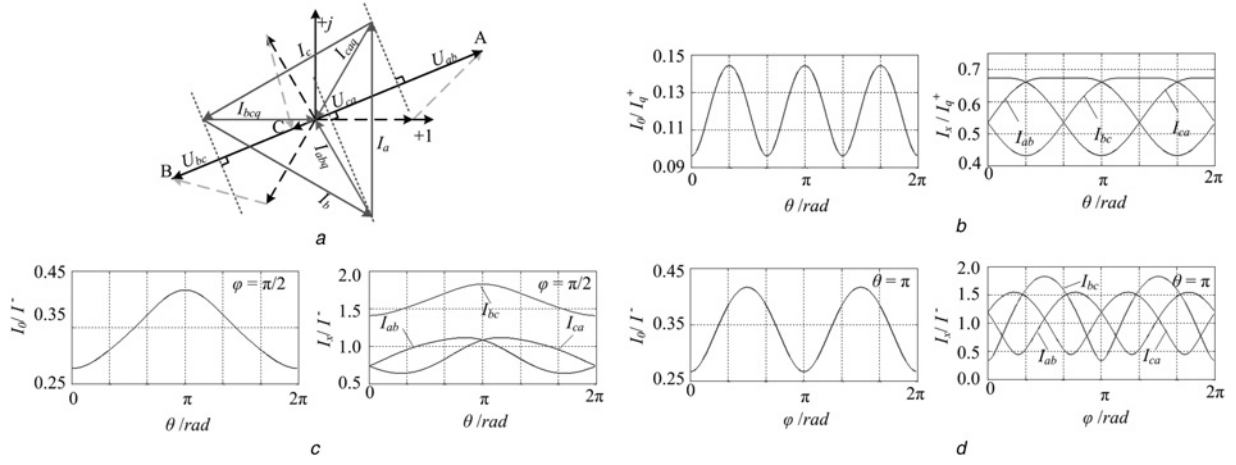


**Fig. 3** Discussion of circulating current  
a Phasors diagram when  $k$  equals to 1  
b Amplitudes of circulating and phase currents  
c Amplitudes of circulating and phase currents when  $\varphi$  is  $\pi/2$   
d Amplitudes of circulating current and phase currents when  $\theta$  is  $\pi$

$I_{bc}$ ,  $I_{ca}$  can be expressed as

$$\begin{bmatrix} I_{ab} \\ I_{bc} \\ I_{ca} \end{bmatrix} = \begin{bmatrix} \frac{1}{2}I_d^+ + \frac{1}{2}I_d^- + \frac{\sqrt{3}}{6}I_q^- + X \\ -\frac{\sqrt{3}}{3}I_q^- + X \\ -\frac{1}{2}I_d^+ - \frac{1}{2}I_d^- + \frac{\sqrt{3}}{6}I_q^- + X \end{bmatrix} + j \begin{bmatrix} \frac{\sqrt{3}}{6}I_d^+ - \frac{\sqrt{3}}{6}I_d^- + \frac{1}{2}I_q^- + Y \\ -\frac{\sqrt{3}}{3}I_d^+ + \frac{\sqrt{3}}{3}I_d^- + Y \\ \frac{\sqrt{3}}{6}I_d^+ - \frac{\sqrt{3}}{6}I_d^- - \frac{1}{2}I_q^- + Y \end{bmatrix} \quad (13)$$

After selecting a proper circulating current phasor  $I_0$ ;  $I_{ab}$ ,  $I_{bc}$ ,  $I_{ca}$  can be vertical with  $U_{ab}$ ,  $U_{bc}$ ,  $U_{ca}$ , respectively. To maintain the overall active power balanced, amplitude of positive-sequence active current  $I_d^+$  can be solved as

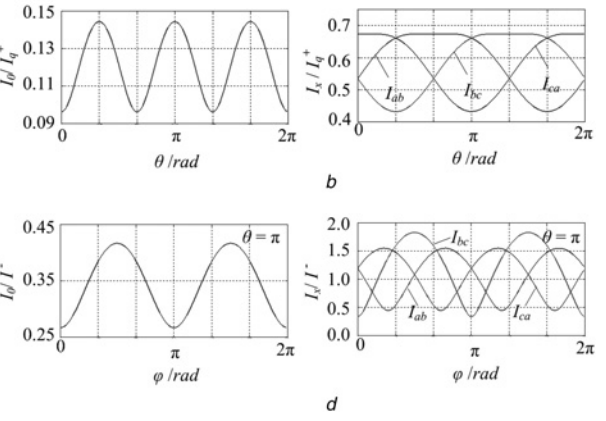
$$I_d^+ = -\frac{U_d^- I_d^- + U_q^- I_q^-}{U_d^+} \quad (14)$$

Note that the amplitude of positive-sequence active current  $I_d^+$  will become zero under conditions of balanced voltages or line currents.

According to (10), the expression of circulating current phasor is obtained (see (15))

### 3.3 Comprehensive compensation

In this mode, positive-sequence reactive power currents and negative-sequence currents are compensated by STATCOM simultaneously. From the analysis above, there exists a proper circulating current component which can be utilised to redistribute the different active power components produced by positive-sequence reactive currents and negative-sequence currents. According to the superposition theorem, when STATCOM works



in comprehensive compensation mode, the circulating current phasor required is the summation of the two circulating current phasors as shown in (12) and (15). Meanwhile, to maintain the overall dc power balance, the currents and voltages should also meet the constraints as shown in (14).

### 3.4 Discussion of circulating current

Circulating current will be discussed based on the derived expression. It can be known from (12) and (15) that the circulating current is determined by the voltages and currents. Defining  $k$  is the voltage unbalance degree, and  $k = U^-/U^+$ . From (12) and (15), it can be proven that the denominator will become zero if  $k$  equals to 1 which leads to an infinite circulating current, in this condition STATCOM could hardly compensate reactive and negative-sequence currents. It is interesting to find that the circulating current approaching infinity is a consequence of line voltages; two of the line voltage phasors have the same phase and another one has the opposite angle when  $U^-$  is equal to  $U^+$ , in this condition the three line voltage phasors are in one line as shown in Fig. 3a. Therefore, it is hard to find a suitable circulating current phasor  $I_0$ , since  $I_{ab}$ ,  $I_{bc}$ ,  $I_{ca}$  should be parallel with each other if  $I_{ab}$ ,  $I_{bc}$ ,  $I_{ca}$  are orthogonal with  $U_{ab}$ ,  $U_{bc}$ ,  $U_{ca}$ , respectively.

In fact, the analysis of maximum current through the cluster is useful to define the required current capability of STATCOM during a certain unbalanced degree, and for example, the condition that  $k$  is 20% is discussed. Substituting (12) into (9), it can be seen that the circulating current has maximum value in reactive current compensation mode when negative-sequence voltage angle  $\theta$  is  $\pi$ /

**Table 1** Main parameters of cascaded STATCOM

Parameter	Value
grid line voltage, V	380
cascaded number	2
arm inductance ( $L$ ), mH	1
sub-module capacitor ( $C$ ), mF	5
carrier frequency ( $f_c$ ), kHz	5
reference value of dc voltage, V	340

$$I_0 = \frac{U_d^+ U_d^+ I_q^- - U_d^+ U_d^- I_q^- + U_d^+ U_q^- I_d^+ - U_d^+ U_q^- I_d^- - U_d^- U_q^- I_d^+ - U_d^- U_q^- I_d^-}{\sqrt{3}(U_d^- U_d^- - U_d^+ U_d^+ + U_q^- U_q^-)} + j \frac{U_d^+ U_d^+ I_d^- + U_d^+ U_d^- I_d^+ + U_d^+ U_d^- I_d^- - U_d^+ U_q^- I_q^- + U_d^- U_d^- I_d^+ - U_q^- U_q^- I_d^-}{\sqrt{3}(U_d^- U_d^- - U_d^+ U_d^+ + U_q^- U_q^-)} \quad (15)$$

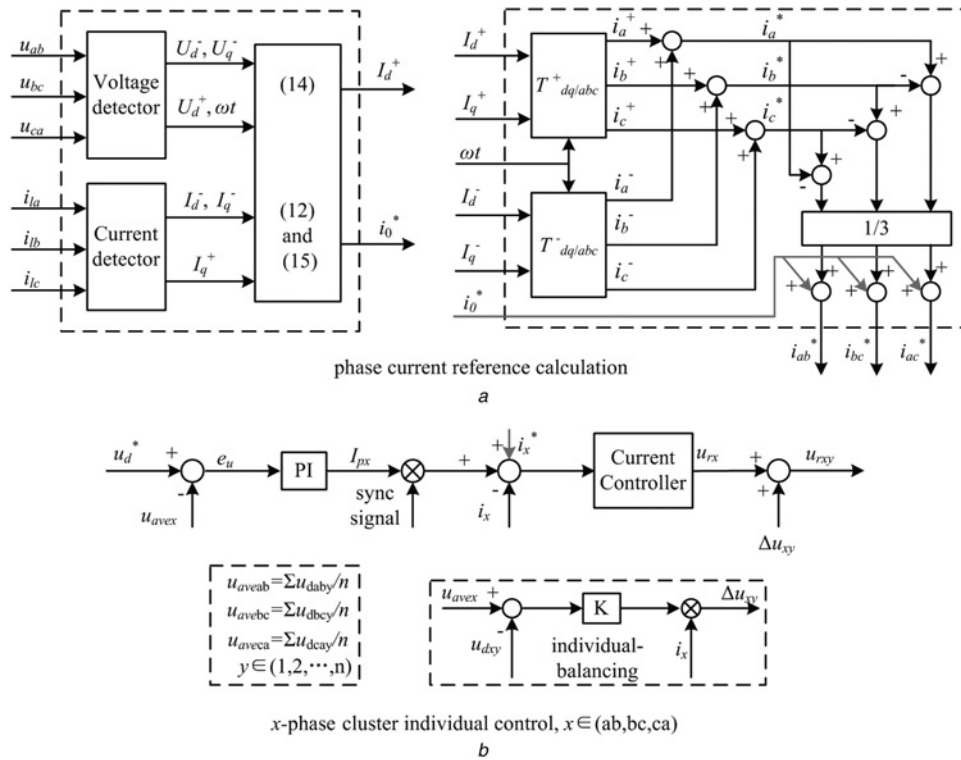
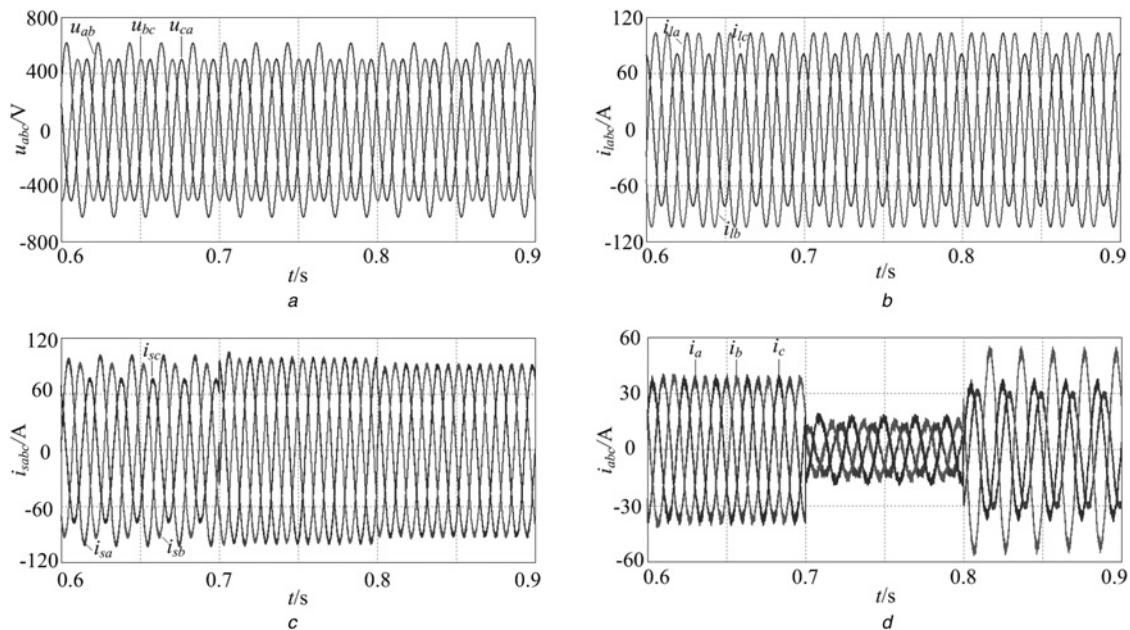


**Fig. 4** Comprehensive compensation method for cascaded STATCOM

a Phase current reference calculation  
 b Cluster individual control

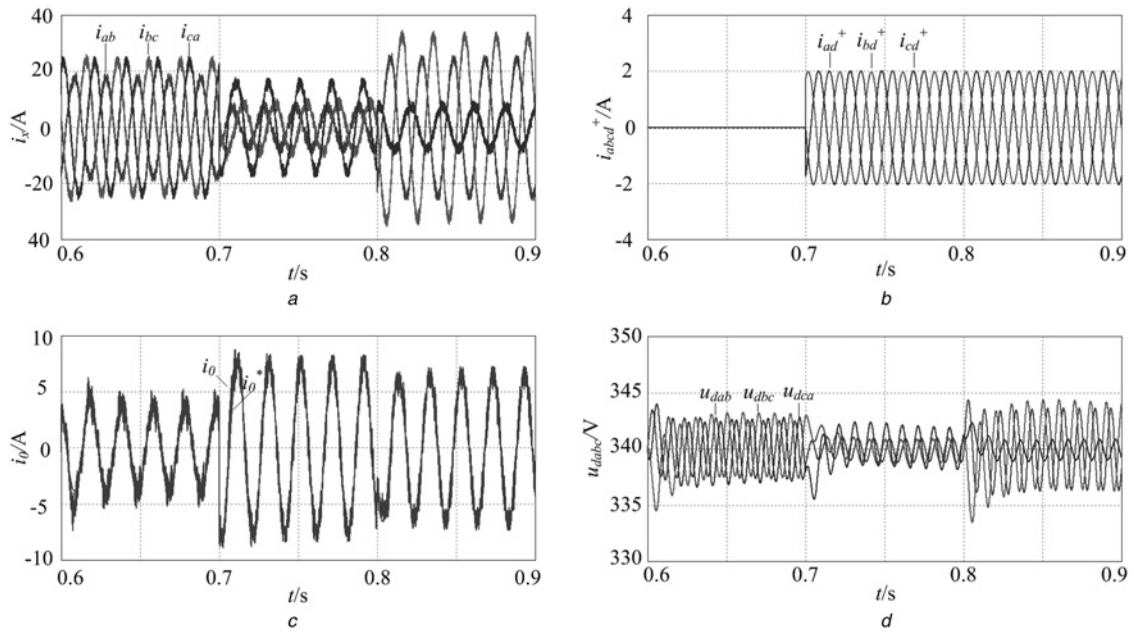
3,  $\pi$  and  $5\pi/3$ , the amplitudes of circulating current and phase currents with  $\theta$  varies from 0 to  $2\pi$  are shown in Fig. 3b, and the maximum value of  $I_{\max}/I_q^+$  and  $I_0/I_q^+$  are 0.6745 and 0.1443, respectively. Combining (13) and (15), it can be known that the circulating current has multiple maximum values in negative-sequence current compensation mode when  $\theta$  is  $\pi$ .

Fig. 3c shows the amplitudes of circulating current and phase currents with negative-sequence voltage angle  $\theta$  varies from 0 to  $2\pi$  when  $\varphi$  is  $\pi/2$ . While Fig. 3d shows the amplitudes of circulating current and phase currents with negative-sequence current angle  $\varphi$  varies from 0 to  $2\pi$  when  $\theta$  is  $\pi$ , the maximum ratio of  $I_{\max}/I$  and  $I_0/I$  are 1.8273 and 0.4167.



**Fig. 5** Compensation performance of STATCOM

a Grid phase voltages  
 b Load currents  
 c Grid side currents  
 d Line currents of STATCOM



**Fig. 6** Simulation wave of STATCOM

- a Phase currents of STATCOM
- b References of active power currents
- c Circulating current
- d Capacitor voltages of three-phase clusters

#### 4 Comprehensive compensation method for STATCOM

On the basis of the expression of circulating current derived in Section 3, a comprehensive compensation method for delta-connected STATCOM is proposed in this section, which includes grid voltages and load currents detection, phase current reference calculation and cluster individual control as shown in Fig. 4.

The voltage and current detector based on a second-order generalised integrator proposed in [34] provides an effective solution for grid synchronisation, and positive- and negative-sequence detections. This method is also employed in this paper to detect the grid voltage signals  $U_d^+$ ,  $U_d^-$ ,  $U_q^-$ ,  $\omega t$  and load current signals  $I_q^+$ ,  $I_d^-$  and  $I_q^-$ . With those voltage and current signals detected, the reference of circulating current  $i_0^*$  and positive-sequence active power current  $I_d^+$  can be calculated according to (12), (14) and (15). Meanwhile, the line current

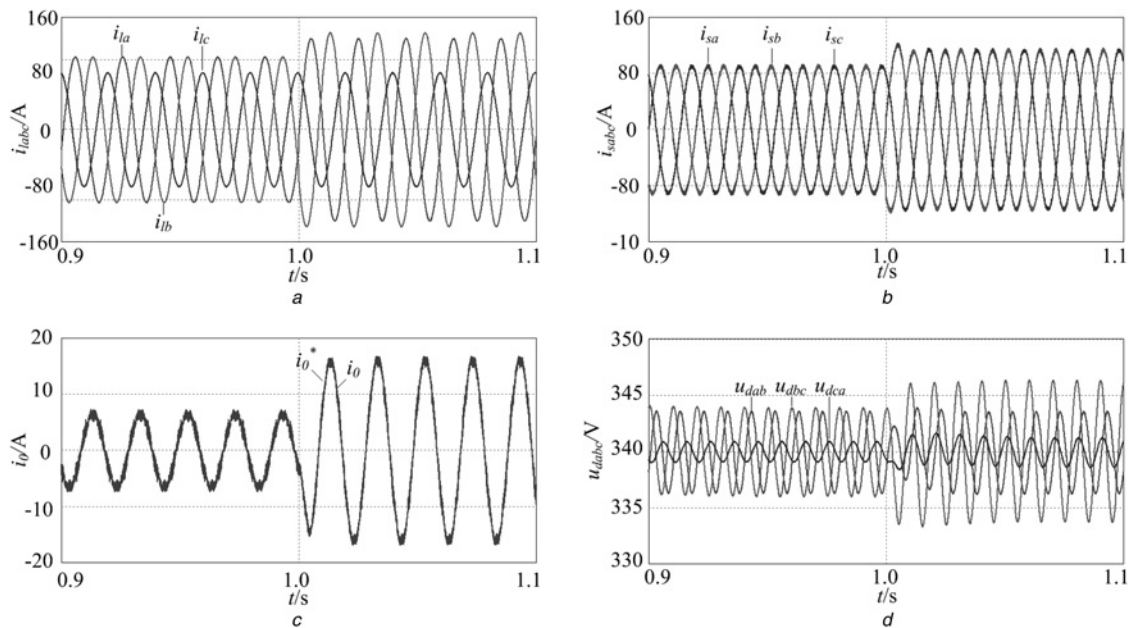


**Fig. 7** Simulation wave of STATCOM under unbalanced load step

- a Load currents
- b Grid side currents
- c Circulating current and its reference
- d Capacitor voltages of three-phase clusters

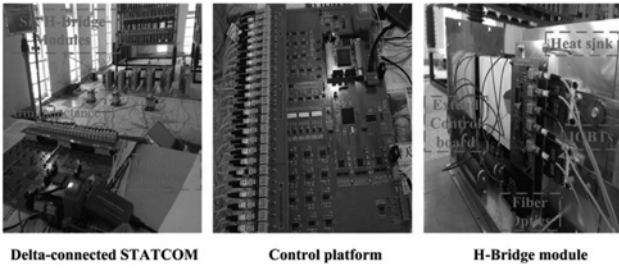


Fig. 8 Experimental prototype of delta-connected STATCOM

references  $i_a^*$ ,  $i_b^*$  and  $i_c^*$  can also be calculated through positive- and negative-sequence  $dq/abc$  transformation of  $I_d^+$ ,  $I_q^+$  and  $I_d^-$ ,  $I_q^-$ . Then, three-phase current references  $i_{ab}^*$ ,  $i_{bc}^*$  and  $i_{ca}^*$  can be synthesised by adding the circulating current reference  $i_0^*$  with the line current reference  $i_a^*$ ,  $i_b^*$  and  $i_c^*$  according to (5) as shown in Fig. 4a.

Seen from Fig. 4b, the cluster individual control is composed of average voltage control, current control and individual balancing control. To keep the average dc-link voltage stable, PI controller is adopted. The error  $e_u$  between reference  $u_d^*$  and average voltage  $u_{aver}$  of each cluster is regarded as the input of PI controller, and then the output will be multiplied with the synchronous signal of each line voltage [ $\sin(\omega t + \pi/6 + 2n\pi/3)$  with  $n=0, 1, 2$ ] to adjust the positive-sequence active component of each phase current. To enhance the response performance of STATCOM, deadbeat controller is adopted for the current inner-loop. Individual balancing control is utilised to regulate capacitor voltage of each H-bridge module in each cluster and P controller is used in this control loop. Carrier-phase-shifted PWM (CPS-PWM) is also used

in this paper. Detailed description of individual balancing control and CPS-PWM is shown in [24, 30], respectively.

As shown in Fig. 4, the references of circulating current and phase current are calculated directly based on the instantaneous grid voltages and load currents, which can improve the dynamic behaviour and cluster-balancing control performance especially under unbalanced conditions. Moreover, the compensation performance can also be improved since cluster-balancing control is achieved only by circulating current in the proposed control method; while, addition negative-sequence current maybe produced by voltage control loop in the individual phase current control strategy.

## 5 Simulation and experimental results

### 5.1 Simulation results

To evaluate the performance of the proposed control method, a simulated model of delta-connected cascaded STATCOM is established. Parameters of simulation are listed in Table 1.

As shown in Fig. 1, three-phase balance resistance and inductance loads ( $L_1 = 4$  mH,  $R_1 = 3$   $\Omega$ ) and a single-phase resistance load ( $R_2 = 18$   $\Omega$ ) connected between phases A and B are adopted to simulate the unbalanced loads. To verify the control method, three compensation modes are simulated. The voltage unbalance degree  $k$  is 15% in this simulation.

Unbalanced grid line voltages are shown in Fig. 5a. The unbalanced loads are switched on at  $t=0.5$  s, load currents are shown in Fig. 5b, which contain positive-sequence reactive and negative-sequence currents. Grid side currents are shown in Fig. 5c, from 0.6 to 0.7 s, positive-sequence reactive currents are compensated; from 0.7 to 0.8 s, negative-sequence currents are compensated; after  $t=0.8$  s, these currents are compensated

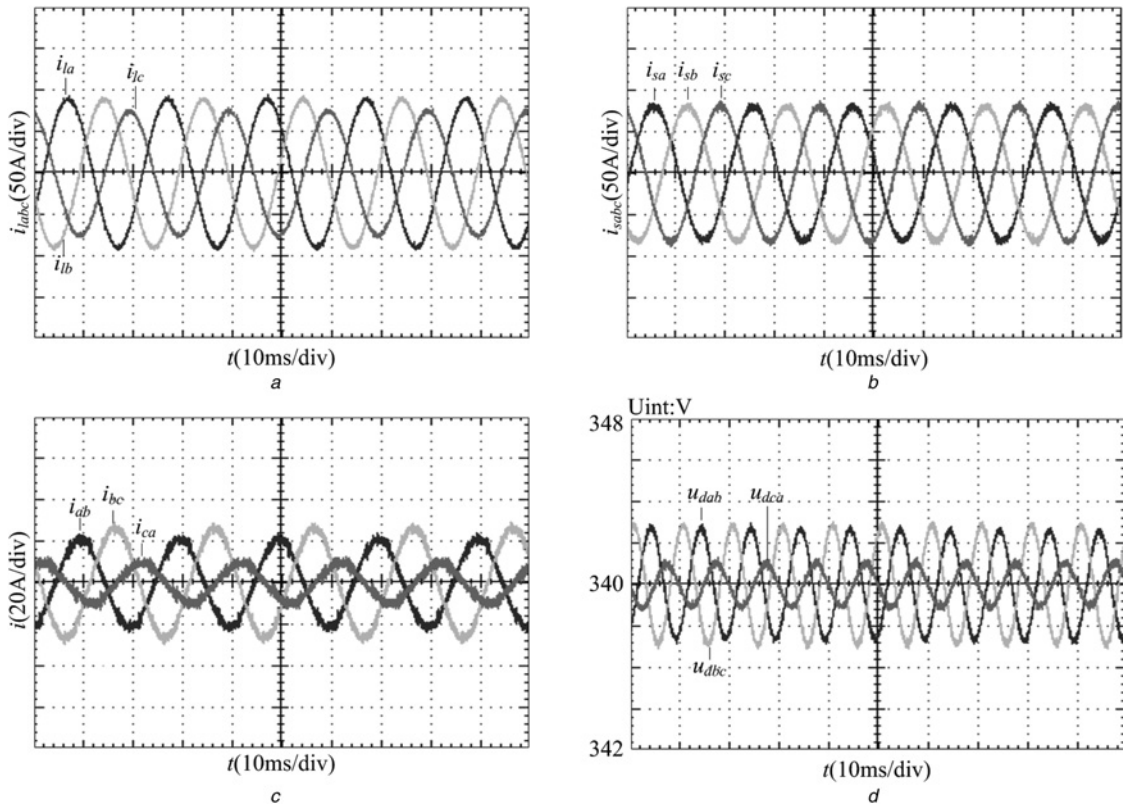
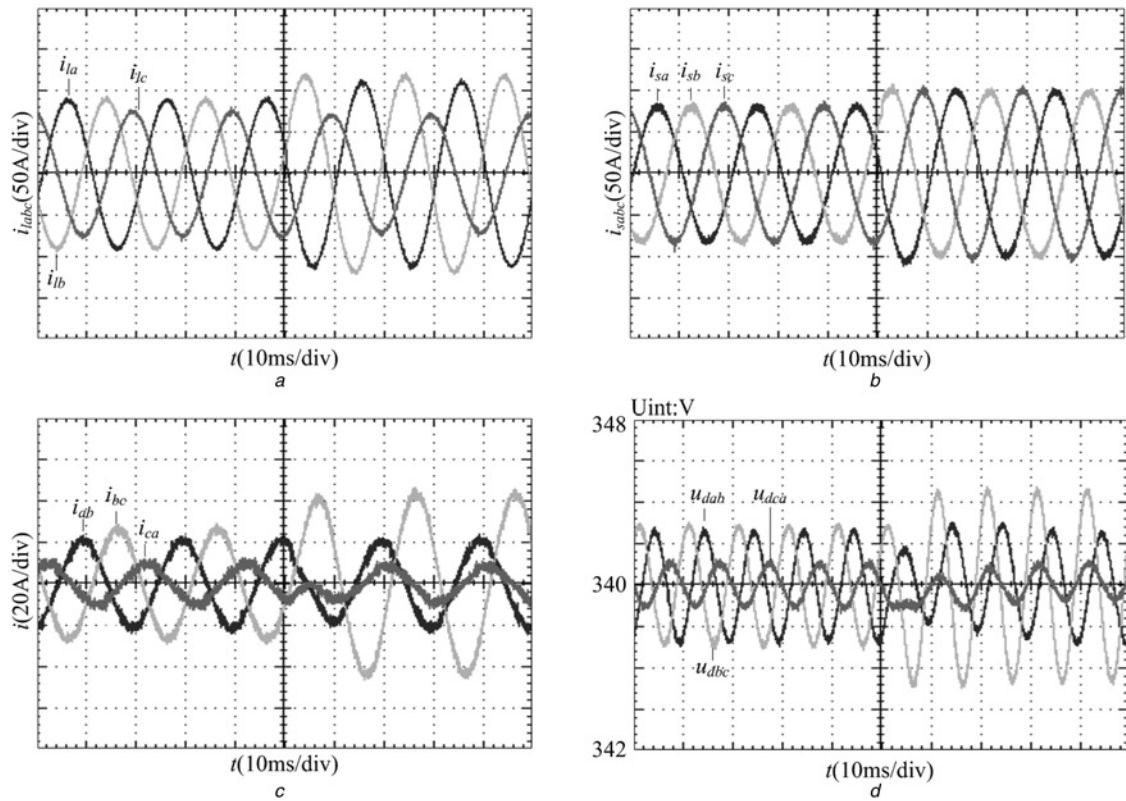


Fig. 9 Experiment wave of delta-connected STATCOM

- a Load currents
- b Grid side currents
- c Phase currents of STATCOM
- d Capacitor voltages of three-phase clusters



**Fig. 10** Experiment wave of delta-connected STATCOM during the load transition

- a Load currents
- b Grid side currents
- c Phase currents of STATCOM
- d Capacitor voltages of three-phase clusters

comprehensively. Line currents of STATCOM are shown in Fig. 5d, the line currents are balanced in 0.6–0.7 s, and the grid side PF is improved from 0.92 to 0.99 after that positive-sequence reactive currents are compensated. While, the line currents become unbalanced in 0.7–0.8 s, because addition active power currents are introduced in line currents. After negative-sequence currents are compensated, the unbalanced degree of grid side currents is reduced rapidly from 14.9 to 0.3%. After  $t=0.8$  s, reactive power and negative-sequence currents are compensated simultaneously, as a result the PF is raised near to 1 and unbalanced degree is decreased approximately to zero, then a good compensation performance is achieved.

Phase currents of STATCOM are shown in Fig. 6a, since circulating current was employed to transfer active power between clusters, the phase currents are unbalanced. Addition active power currents are introduced to keep total dc power balanced when negative-sequence currents are compensated and its references are shown in Fig. 6b. Fig. 6c shows circulating current and its reference, a good tracking performance is obtained. From Fig. 6d, it can be known that all the dc-link voltages of three clusters are stable and balanced during this process, so the voltage balancing control of STATCOM is achieved.

To test the dynamic performance of system, single-phase load is plunged on at  $t=1.0$  s, then the loads become unbalanced. The performance of STATCOM in response to loads change is illustrated in Fig. 7. Unbalanced load currents are shown in Fig. 7a. As shown in Fig. 7b, the grid side currents turns to be symmetrical within about a grid period after loads changed. Fig. 7c shows the circulating current and its reference. The capacitor voltages are maintained balanced during this transient as shown in Fig. 7d. From Figs. 5 to 7, it can be concluded that the proposed method is feasible no matter the loads are balanced or unbalanced.

## 5.2 Experimental results

An experimental prototype of five-level STATCOM is established. Asymmetrical voltage is made by a  $1.1 \Omega$  resistor connected in phase C. The other main parameters are the same as the simulation. The main circuit and controller of prototype are shown in Fig. 8. Two core controllers DSP-TMS320F2812 and FPGA-EP2C8 are used.

The three-phase balanced loads are switched on first. Experimental results are shown in Fig. 9. Load currents are shown in Fig. 9a; there are lots of reactive and negative-sequence components. Reactive and negative-sequence currents are compensated comprehensively by STATCOM. After compensation, the grid side currents tend to be balanced as shown in Fig. 9b. Unbalanced degree of three-phase grid currents is reduced rapidly, and PF is about 0.99. Phase currents and dc-link capacitor voltages are shown in Figs. 9c and d, respectively. It can be seen that voltage balancing control and comprehensive compensation are achieved.

Switching the single-phase load into system, load currents changed as shown in Fig. 10a. Grid side currents and phase currents of STATCOM are shown in Figs. 10b and c. It can be seen that the reactive power components and negative-sequence components of load current are compensated after a transient when the loads changed. The dc-link voltages of three-phase clusters were well controlled during load transition as shown in Fig. 10d.

## 6 Conclusions

The analytical expression of circulating current is derived based on the phasors analysis of current and voltage, when delta-connected STATCOM operates under asymmetrical voltage conditions, and a

comprehensive compensation method for delta-connected STATCOM is proposed. Simulation and experiments have been made and the results show that the reactive power and negative-sequence components of load currents were compensated, as a result the PF and unbalance degree of grid side currents were improved rapidly. Meanwhile, cluster-balancing control was also achieved with this method. Therefore, it can be concluded that the performance of the proposed method shows clear advantage in the presence of asymmetrical voltage and unbalanced loads.

## 7 References

- 1 Muñoz, J.A., Espinoza, J.R., Baier, C.R., *et al.*: 'Decoupled and modular harmonic compensation for multilevel STATCOMs', *IEEE Trans. Ind. Electron.*, 2014, **61**, (6), pp. 2743–2753
- 2 Han, H., Yang, Z.N., Chen, B., *et al.*: 'Evaluation of cascade multilevel converter based STATCOM for arc furnace flicker mitigation', *IEEE Trans. Ind. Appl.*, 2007, **43**, (2), pp. 378–385
- 3 Lee, T.L., Hu, S.H., Chan, Y.H.: 'D-STATCOM with positive-sequence admittance and negative-sequence conductance to mitigate voltage fluctuations in high-level penetration of distributed-generation systems', *IEEE Trans. Ind. Electron.*, 2013, **60**, (4), pp. 1417–1428
- 4 Kouro, S., Malinowski, M., Gopakumar, K., *et al.*: 'Recent advances and industrial applications of multilevel converters', *IEEE Trans. Ind. Electron.*, 2010, **57**, (8), pp. 2553–2580
- 5 Malinowski, M., Gopakumar, K., Rodriguez, J., *et al.*: 'A survey on cascaded multilevel inverters', *IEEE Trans. Ind. Electron.*, 2010, **57**, (7), pp. 2097–2206
- 6 Song, W.C., Huang, A.Q.: 'Fault-tolerant design and control strategy for cascaded H-bridge multilevel converter-based STATCOM', *IEEE Trans. Ind. Electron.*, 2010, **57**, (8), pp. 2259–2269
- 7 Gultekin, B., Ermis, M.: 'Cascaded multilevel converter-based transmission STATCOM: system design methodology and development of a 12 kV  $\pm$  12 MVar power stage', *IEEE Trans. Power Electron.*, 2013, **28**, (11), pp. 4930–4950
- 8 Du, S.X., Liu, J.J., Lin, J.L., *et al.*: 'A novel DC voltage control method for STATCOM based on hybrid multilevel H-Bridge converter', *IEEE Trans. Power Electron.*, 2009, **24**, (1), pp. 45–58
- 9 Townsend, C.D., Summers, T.J., Betz, R.E.: 'Impact of practical issues on the harmonic performance of phase-shifted modulation strategies for a cascaded H-Bridge StatCom', *IEEE Trans. Ind. Electron.*, 2014, **61**, (6), pp. 2655–2664
- 10 Napoles, J., Watson, A.J., Padilla, J.J., *et al.*: 'Selective harmonic mitigation technique for cascaded H-Bridge converters with nonequal DC link voltages', *IEEE Trans. Ind. Electron.*, 2013, **60**, (5), pp. 1963–1971
- 11 Rodriguez, J., Correa, P., Silva, C.: 'A vector control technique for medium-voltage multilevel inverters', *IEEE Trans. Ind. Electron.*, 2002, **49**, (4), pp. 882–888
- 12 Farivar, G., Hredzak, B., Agelidis, V.G.: 'Reduced-capacitance thin-film H-bridge multilevel STATCOM control utilizing an analytic filtering scheme', *IEEE Trans. Ind. Electron.*, 2015, **62**, (10), pp. 6457–6468
- 13 Alvarenga, M.B.de., Pomilio, J.A.: 'Voltage balancing and commutation suppression in symmetrical cascade multilevel converters for power quality applications', *IEEE Trans. Ind. Electron.*, 2014, **61**, (11), pp. 5996–6003
- 14 Lee, C.-T., Chen, H.-C., Yang, C.-H., *et al.*: 'A flexible dc voltage balancing control based on the power flow management for star-connected cascaded H-bridge converter'. IEEE Energy Conversion Congress and Exposition (ECCE), Pittsburgh, PA, September 2014, pp. 3922–3929
- 15 Xu, R., Yu, Y., Yang, R.F., *et al.*: 'A novel control method for transformer-less H-bridge cascaded STATCOM with star configuration', *IEEE Trans. Power Electron.*, 2015, **30**, (3), pp. 1189–1202
- 16 Akagi, H.: 'Classification, terminology, and application of the modular multilevel cascade converter (MMCC)', *IEEE Trans. Power Electron.*, 2011, **26**, (11), pp. 3119–3130
- 17 Peng, F.Z., Lai, J.S.: 'Dynamic performance and control of a static var generator using cascade multilevel inverters', *IEEE Trans. Ind. Appl.*, 1997, **33**, (3), pp. 748–755
- 18 Peng, F.Z., Wang, J.: 'A universal STATCOM with delta-connected cascade multilevel inverter'. Annual IEEE Power Electronics Specialists Conf., Aachen, Germany, June 2004, pp. 3529–3533
- 19 Sano, K., Takasaki, M.: 'A transformerless D-STATCOM based on a multi-voltage cascade converter requiring no DC sources', *IEEE Trans. Power Electron.*, 2012, **27**, (6), pp. 2783–2795
- 20 Akagi, H., Inoue, S., Yoshii, T.: 'Control and performance of a transformerless cascade PWM STATCOM with star configuration', *IEEE Trans. Ind. Appl.*, 2007, **43**, (4), pp. 1041–1049
- 21 Haw, L.K., Dahidah, M.S.A., Almurib, H.A.F.: 'A new reactive current reference algorithm for the STATCOM system based on cascaded multilevel inverters', *IEEE Trans. Power Electron.*, 2015, **30**, (7), pp. 3577–3588
- 22 Barrena, J.A., Marroyo, L., Vidal, M.A.R., *et al.*: 'Individual voltage balancing strategy for PWM cascaded H-Bridge converter-based STATCOM', *IEEE Trans. Ind. Electron.*, 2008, **55**, (1), pp. 21–29
- 23 Vazquez, S., Leon, J.I., Carrasco, J.M., *et al.*: 'Analysis of the power balance in the cells of a multilevel cascaded H-Bridge converter', *IEEE Trans. Ind. Electron.*, 2010, **57**, (7), pp. 2287–2296
- 24 Ota, J.I.Y., Shibano, Y., Niimura, N., *et al.*: 'A phase-shifted- PWM D-STATCOM using a modular multilevel cascade converter (SSBC) – part I: modeling, analysis, and design of current control', *IEEE Trans. Ind. Appl.*, 2015, **51**, (1), pp. 279–288
- 25 Lee, C.T., Wang, B.S., Chen, S.W., *et al.*: 'Average power balancing control of a STATCOM based on the cascaded H-Bridge PWM converter with star configuration', *IEEE Trans. Ind. Appl.*, 2014, **50**, (6), pp. 3893–3901
- 26 Behrouzian, E., Bongiorno, M., Parra, H.Z.D.L.: 'Investigation of negative sequence injection capability in H-bridge multilevel STATCOM'. 16th European Conf. on Power Electronics and Applications, Lappeenranta, Finland, August 2014, pp. 1–10
- 27 Hatano, N., Ise, T.: 'Control scheme of cascaded H-bridge STATCOM using zero-sequence voltage and negative-sequence current', *IEEE Trans. Power Deliv.*, 2010, **25**, (2), pp. 543–550
- 28 Zang, C.Y., Liu, Z.: 'Advanced compensation mode for cascade multilevel static synchronous compensator under unbalanced voltage', *IET Power Electron.*, 2015, **8**, (4), pp. 610–617
- 29 Song, Q., Liu, W.H.: 'Control of a cascaded STATCOM with star configuration under unbalanced conditions', *IEEE Trans. Power Electron.*, 2009, **24**, (1), pp. 45–58
- 30 Hagiwara, M., Maeda, R., Akagi, H.: 'Negative-Sequence reactive-power control by a PWM STATCOM based on a modular multilevel cascade converter (MMCC-SDBC)', *IEEE Trans. Ind. Appl.*, 2012, **48**, (2), pp. 720–729
- 31 Betz, R.E., Summers, T.J., Furney, T.: 'Symmetry compensation using a H-bridge multilevel STATCOM with zero sequence injection'. 2006 IEEE Industry Applications Conf. 41st IAS Annual Meeting, Tampa, FL, October 2006, pp. 1724–1731
- 32 Betz, R.E., Summers, T.J.: 'Using a cascaded H-bridge STATCOM for rebalancing unbalanced voltages'. Proc. Seventh Int. Conf. Power Electronics, Daegu, October 2007, pp. 1219–1224
- 33 Yuan, Z., Xia, T.: 'Optimal control strategy for cascaded STATCOM under unsymmetrical power system conditions'. Int. Conf. on Power Electronics and Motion Control Conf., Harbin, China, June 2012, pp. 2721–2726
- 34 Rodriguez, P., Timbus, A.V., Teodorescu, R., *et al.*: 'Flexible active power control of distributed power generation systems during grid faults', *IEEE Trans. Ind. Electron.*, 2007, **54**, (5), pp. 2583–2592